J. Fluid Mech. (2007), *vol.* 586, *pp.* 249–258. © 2007 Cambridge University Press
doi:10.1017/S0022112007007148 Printed in the United Kingdom

Stokes' second flow problem in a high-frequency limit: application to nanomechanical resonators

VICTOR YAKHOT AND CARLOS COLOSQUI

Department of Aerospace and Mechanical Engineering,
Boston University, Boston, MA 02215, USA

(Received 25 March 2007 and in revised form 5 June 2007)

Solving the Boltzmann–BGK equation, we investigate a flow generated by an infinite plate oscillating with frequency ω. The geometrical simplicity of the problem allows a solution in the entire range of dimensionless frequency variation $0 \leqslant \omega\tau \leqslant \infty$, where τ is a properly defined relaxation time. A transition from viscoelastic behaviour of a Newtonian fluid ($\omega\tau \to 0$) to purely elastic dynamics in the limit $\omega\tau \to \infty$ is discovered. The relation of the derived solutions to nanofluidics is demonstrated on a solvable example of a 'plane oscillator'. The results from the derived formulae compare well with experimental data on various nanoresonators operating in a wide range of both frequency and pressure variation.

1. Introduction

During the last two centuries, the Newtonian fluid approximation has been remarkably successful in explaining a wide variety of natural phenomena ranging from flows in pipes, channels and boundary layers to the recently discovered processes in meteorology, aerodynamics, MHD and cosmology. With the advent of powerful computers and the development of effective numerical methods, Newtonian hydrodynamics remains the foundation of various design tools widely used in mechanical and civil engineering. Since technology in the past dealt with large (macroscopic) systems varying on the length and time scales L and T, the Newtonian fluid approximation, typically defined by the smallness of the Knudsen and Weisenberg numbers $Kn = \lambda/L \ll 1$ and $Wi = \tau/T \approx (\lambda/L)(u/c) = KnMa \ll 1$, where $Ma = u/c$ is the Mach number, was accurate enough. The length and time scales λ and $\tau \approx \lambda/c$, are the mean-free path and relaxation time, respectively.

With recent rapid developments in nanotechnology and bioengineering, quantitative descriptions of high-frequency oscillating microflows, i.e. flows where the Newtonian approximation breaks down, have become an important and urgent task from both basic and applied science viewpoints. Modern micro- (nano)electromechanical devices (MEMS and NEMS), operating in the high-frequency range up to $\omega/2\pi = O(10^8 - 10^9$ Hz) ($Wi = \omega\tau \geqslant 1$), can be used for small biological mass detection, subatomic microscopy, viscometry and other applications (Service 2006; Cleland & Roukes 1998; Binning, Quate & Gerber 1986; Ekinci, Huang & Roukes 2004; Verbridge *et al.* 2006). The manufactured devices are so small and sensitive that adsorption of even tiny particles on their surfaces leads to a detectable response in the resonator frequency peak (shift), enabling these revolutionary applications. Since both the frequency shift and width of the resonance peak depend upon properties of the resonator-generated flows, the microresonators may serve as sensors enabling

https://doi.org/10.1017/S0022112007007148 Published online by Cambridge University Press

accurate investigation of fundamental processes in microflows. Often, oscillating flows are a source of new and unexpected phenomena. For example, in a study of the high-frequency electromagnetic-field-driven nano-resonators of linear dimensions $h \times w \times L \approx 0.2 \times 0.7 \times 10\,\mu\text{m}$; K. L. Ekinci & L. M. Karabacak (2006, personal communication) observed a transition in the frequency dependence of the inverse quality factor from $1/Q \approx \gamma/\omega \propto 1/\sqrt{\omega}$, expected in the hydrodynamic limit, to $1/Q \propto 1/\omega$ in the high-frequency (kinetic) limit. Since γ is proportional to the energy dissipation rate (W) into a surrounding gas, the effect discovered points to a frequency-independent dissipation rate W. No quantitative theory describing this transition has been developed.

2. The Boltzmann–BGK equation

Interested in the rapidly oscillating flows, where the Navier–Stokes equations break down, we consider the kinetic equation in the relaxation time approximation (RTA):

$$\frac{\partial f}{\partial t} + \boldsymbol{v}\cdot\nabla f = \mathscr{C}. \tag{2.1}$$

In accord with Boltzmann's H-theorem, the initially non-equilibrium gas must monotonically relax to thermodynamic equilibrium. This leads to the relaxation time anzatz, qualitatively satisfying this requirement:

$$\mathscr{C} \approx -\frac{f - f^{eq}}{\tau(f)}. \tag{2.2}$$

In the mean-field approximation, valid close to equilibrium where all gradients are small, $\tau(f) = \tau = \text{const}$. In what follows we set the Boltzmann constant $k_B = 1$ and define temperature as $\theta = \overline{(\boldsymbol{v} - \boldsymbol{u})^2}/d$, where $\overline{\boldsymbol{v}} = \boldsymbol{u}$ and d stands for the space dimensionalty. This equation, with $f^{eq} = \rho/(2\pi\theta)^{3/2}\exp(-(\boldsymbol{v}-\boldsymbol{u})^2/2\theta)$, often considered as a generic equation of fluid dynamics, is the celebrated Boltzmann–BGK equation widely used for both theoretical and numerical (Lattice Boltzmann Methods) studies of non-equilibrium fluids (Bhatnagar, Gross & Krook 1954; Chen & Doolen 1998; Chen *et al.* 2003; Benzi, Succi & Vergassola 1992).

The Chapman–Enskog expansion of BGK. Multiplying (2.1), (2.2) by v and integrating over $\boldsymbol{v}$ gives

$$\frac{\partial u_i}{\partial t} + u_j\frac{\partial u_i}{\partial x_j} + \frac{1}{\rho}\frac{\partial}{\partial x_i}\sigma_{ij} = 0 \tag{2.3}$$

where the stress tensor, written for $i \neq j$ is

$$\sigma_{ij} = \rho\overline{(v_i - u_i)(v_j - u_j)} \equiv \int \mathrm{d}\boldsymbol{v}(v_i - u_i)(v_j - u_j)f(\boldsymbol{v}, \boldsymbol{x}, t). \tag{2.4}$$

Usually, evaluation of the stress tensor is a difficult task. The simplified system (2.1)–(2.2) for a single-particle distribution function allows calculation of nonlinear contributions to the momentum stress tensor $\sigma_{ij} = \overline{(v_i - u_i)(v_j - u_j)} - \overline{v^2}\delta_{ij}/d$. In a remarkable paper, based on (2.1)–(2.2), Chen *et al.* (2004) formulated the Chapman–Enskog expansion in powers of two dimensionless parameters: $Kn = \lambda/\delta_-$, where δ_- is the width of the boundary layer, and $Wi = \tau\omega = \tau(\partial_t u)/u$. In this formulation: $\nabla = \epsilon\nabla_1$,

$$\frac{\partial}{\partial t} = \epsilon\frac{\partial}{\partial t_0} + \epsilon^2\frac{\partial}{\partial t_1} + \epsilon^3\frac{\partial}{\partial t_2} + \cdots \tag{2.5}$$

https://doi.org/10.1017/S0022112007007148 Published online by Cambridge University Press

and the probability density function (p.d.f.) is expanded in powers of ϵ as $f = f^{(0)} + \epsilon f^{(1)} + \epsilon^2 f^{(2)} + \cdots$. Substituting these expressions into (2.1), (2.2) and equating terms of the same order in ϵ results in $f^{(0)} = f^{eq}$ and

$$\left(\frac{\partial}{\partial t_0} + \boldsymbol{v}\cdot\nabla\right) f^{(0)} = -\frac{f^{(1)}}{\tau}, \tag{2.6}$$

$$\left(\frac{\partial}{\partial t_0} + \boldsymbol{v}\cdot\nabla\right) f^{(1)} + \frac{\partial}{\partial t_1} f^{(0)} = -\frac{f^{(2)}}{\tau}, \tag{2.7}$$

etc. The mean of any fluctuating variable is then calculated as $\overline{A(\boldsymbol{v})} = A^{(0)} + A^{(1)} + A^{(2)} + \cdots$, where $A^{(n)} = \int f^{(n)} A(\boldsymbol{v})\, \mathrm{d}\boldsymbol{v}$.

To illustrate the main results and simplify notation, in what follows we set temperature $\theta = \text{const}$. The calculation of Chen *et al.* (2004) gives

$$f^{(1)} \approx -\frac{\tau}{\theta} f^{(0)} S_{ij} \left[(v_i - u_i)(v_j - u_j) - \frac{(\boldsymbol{v}-\boldsymbol{u})^2}{d}\delta_{ij}\right] \tag{2.8}$$

and

$$f^{(2)} = -2\tau^2 f^{(0)} \left[(v_i - u_i)\frac{\partial}{\partial x_j}\left(S_{ij} - \frac{1}{d}\nabla\cdot\boldsymbol{u}\,\delta_{ij}\right) + O((v_p - u_p)(v_q - u_q)S_{pi}S_{qi})\right]. \tag{2.9}$$

It is important to stress that the last contribution to the right-hand side of (2.9) involves even powers of $v' = v - u$ and various products of S_{ij}. The result is (Chen *et al.* 2004)

$$\begin{aligned}\sigma_{ij} = {} & 2\tau\theta S_{ij} - 2\tau\theta(\partial_t + \boldsymbol{u}\cdot\nabla)(\tau S_{ij}) \\ & - 4\tau^2\theta\left[S_{ik}S_{kj} - \frac{1}{d}\delta_{ij}S_{kl}S_{kl}\right] + 2\tau^2\theta[S_{ik}\Omega_{kj} + S_{jk}\Omega_{ki}]\end{aligned} \tag{2.10}$$

where the rate of strain and the vorticity tensor are respectively,

$$\Omega_{ij} = \frac{1}{2}\left[\frac{\partial u_i}{\partial x_j} - \frac{\partial u_j}{\partial x_i}\right], \quad S_{ij} = \frac{1}{2}\left[\frac{\partial u_i}{\partial x_j} + \frac{\partial u_j}{\partial x_i}\right].$$

The first term on the right of (2.10), resulting from the first-order Chapman–Enskog (CE) expansion, corresponds to the familiar Navier–Stokes equations for a Newtonian fluid and the nonlinear (non-Newtonian) corrections, given by the remaining terms, are generated at the next, second order. The constitutive relation (2.10) is quite complex and, in general, can be attacked by numerical methods only. However, it is greatly simplified in an important class of simple unidirectional flows.

3. Stokes' second problem

The flow of a fluid filling half-space $0 \leqslant y$ is generated by a solid plate at $y = 0$ moving along the x-axis with velocity $U_p(0, t) = U\cos\omega t$. Since velocity components in the y- and z-directions are equal to zero, we need only solve the equations for the x-component of velocity field $u(y, t)$. Due to the geometry of the problem

$$u_x \equiv u = u(y, t), \quad u_y \equiv v = 0, \quad \boldsymbol{u}\cdot\nabla = 0, \quad \partial_x = 0. \tag{3.1}$$

Thus, since $i \neq j$, we are interested in $\sigma_{x,y}$. In this case, the equation of motion corresponding to the stress tensor (2.10) is very simple:

$$\frac{\partial u}{\partial t} = \nu\left(1 - \tau\frac{\partial}{\partial t}\right)\frac{\partial^2 u}{\partial y^2}. \tag{3.2}$$

https://doi.org/10.1017/S0022112007007148 Published online by Cambridge University Press

In the limit $\omega\tau \to 0$, this equation is to be solved subject to the no-slip boundary condition, $u(0,t) = U\cos\omega t$, $\lim_{y\to\infty} u(y,t) = 0$. Seeking a solution satisfying the boundary condition at $y \to \infty$ as $u = \mathrm{Re}\,(\phi(y)\mathrm{e}^{-\mathrm{i}\omega t})$ gives $\phi = B\mathrm{e}^{-y/\delta}$ and in the low-frequency limit $Wi = \tau\omega \ll 1$:

$$u(y,t) = U\exp\left(-\sqrt{\frac{\omega}{2\nu}}\left(1-\frac{\tau\omega}{2}\right)y\right)\cos\left(\omega t - \sqrt{\frac{\omega}{2\nu}}\left(1+\frac{\tau\omega}{2}\right)y\right). \tag{3.3}$$

In a classic case $\omega\tau = 0$, the flow is characterized by a single scale $\sqrt{2\nu/\omega}$ describing both 'penetration depth' and wavelength of transverse waves radiated by the oscillating plate. We can see that the non-Newtonian $O(\tau\omega)$ contribution leads to the formation of two different length scales: the $O(\tau\omega)$ increasing penetration depth and the wavelength decreasing by the same magnitude. This is a qualitatively new feature of this flow. Now we calculate the dissipation rate. The force acting on a unit area of the wall at $y = 0$:

$$\mu\left(1-\tau\frac{\partial}{\partial t}\right)\frac{\partial u(0,t)}{\partial y} = -U\sqrt{\omega\mu\rho}\left[\cos\left(\omega t+\frac{\pi}{4}\right)+\frac{\tau\omega}{2}\cos\left(\omega t-\frac{\pi}{4}\right)\right] \tag{3.4}$$

is phase-shifted relative to velocity field $u(0,t) = U\cos\omega t$. This result differs from its classic Newtonian counterpart by an $O(\tau\omega/2)$ shift. The mean energy dissipated per unit time per unit area of the plate is calculated if we multiply (3.4) by $-U\cos\omega t$ and integrate over one cycle, with the result:

$$W(\tau,\omega) = \frac{U^2}{2}\sqrt{\frac{\omega\mu\rho}{2}}\left(1+\frac{\tau\omega}{2}\right) > W(0,\omega). \tag{3.5}$$

4. Large deviations from Newtonian fluid mechanics

As $\tau \to 0$, the expansion gives the classic Stokes results (Stokes 1851; Landau & Lifshitz 1959). Moreover, in the limit $\tau\omega \ll 1$, the second-order-in-$\boldsymbol{S}$ correction to (2.10) disappears due to the symmetries of the problem defined by (3.1). Expression (2.10) includes a time derivative which, for the oscillating flow we are interested in this paper, introduces an additional dimensionless parameter $Wi = \tau\omega$ into the expansion. Therefore, the CE expansion is in fact an expansion in two dimensionless parameters $KnMa = \tau\partial_y u \approx u\lambda/c\delta$ and $Wi = (\tau/u)\partial_t u \approx \tau\omega$. As will be shown below, in simple-geometry oscillating flows, these parameters are quite different: as $\tau\omega \to \infty$, the second parameter $Kn \to 0$. Thus, while neglecting the small, $O(\nabla^{2n}u)$ term with $n > 1$, the 'Burnett contributions', we will attempt to sum the entire series in $Wi = \tau\omega$. The Boltzmann equation is

$$\frac{\partial f}{\partial t} + v_\alpha\frac{\partial f}{\partial x_\alpha} + \frac{f}{\tau} = \frac{f^e}{\tau}. \tag{4.1}$$

Multiplying (4.1) by $(v_i - u_i)(v_j - u_j)$ and integrating over $\boldsymbol{v}$, we derive the equation for the stress tensor $(i \neq j)$:

$$\frac{\partial\sigma_{ij}}{\partial t} + \frac{\sigma_{ij}}{\tau} = -\frac{1}{\rho}\int \mathrm{d}\boldsymbol{v}(v_i-u_i)(v_j-u_j)v_\alpha\frac{\partial f}{\partial x_\alpha} \tag{4.2}$$

or

$$\frac{\partial\sigma_{ij}}{\partial t} + \boldsymbol{u}\cdot\nabla\sigma_{ij} + \frac{\sigma_{ij}}{\tau} = -2\sigma_{i,\alpha}\frac{\partial u_j}{\partial x_\alpha} - \frac{\partial}{\partial x_\alpha}\overline{(v_\alpha-u_\alpha)(v_i-u_i)(v_j-u_j)} - \sigma_{ij}\nabla\cdot\boldsymbol{u}. \tag{4.3}$$

https://doi.org/10.1017/S0022112007007148 Published online by Cambridge University Press

By virtue of (3.1), this equation is simplified:

$$\frac{\partial \sigma_{ij}}{\partial t} + \frac{\sigma_{ij}}{\tau} = -2\sigma_{i,\alpha}\frac{\partial u_j}{\partial x_\alpha} - \frac{\partial}{\partial x_\alpha}\overline{(v_\alpha - u_\alpha)(v_i - u_i)(v_j - u_j)}. \tag{4.4}$$

In the unidirectional flow we are interested in, only $\partial_y u \neq 0$ and therefore, $\sigma_{i,\alpha}\partial_{x_\alpha} u = \sigma_{yy}\partial_y u$. The remaining term on the right of (4.4) can also be simplified, leading to:

$$\frac{\partial \sigma_{y,x}}{\partial t} + \frac{\sigma_{y,x}}{\tau} = -2\theta\frac{\partial u}{\partial y} - \frac{\partial}{\partial y}\overline{v_y^2(v_x - u)} \tag{4.5}$$

where $\theta = \sigma_{y,y} = \overline{v_y^2} = \frac{1}{3}(\boldsymbol{v} - \boldsymbol{u})^2$. This equation is formally exact.

Our goal now is to evaluate

$$\Sigma_{ij} = \frac{\partial}{\partial x_\alpha}\overline{(v_\alpha - u_\alpha)(v_i - u_i)(v_j - u_j)} = \Sigma_{ij}^{(0)} + \Sigma_{ij}^{(1)} + \Sigma_{ij}^{(2)} + \cdots. \tag{4.6}$$

This can be done readily with relations (2.8)–(2.9) derived in Chen *et al.* (2004). We see that $\Sigma_{ij}^{(0)} = 0$ and $\Sigma_{ij}^{(1)} = 0$. Evaluated on $f^{(2)}$ from (2.9):

$$\Sigma_{xy}^{(2)} \approx \tau^2\frac{\partial}{\partial y}\overline{v_y^2(v_x - u_x)^2}|_0\frac{\partial^2 u}{\partial y^2} \approx \tau^2\theta^2\frac{\partial^3 u}{\partial y^3} \tag{4.7}$$

where $\overline{A}|_0 = \int f^0(\boldsymbol{v})A(\boldsymbol{v})\,\mathrm{d}\boldsymbol{v}$. It will be shown *a posteriori* that in both limits $\tau\omega \to 0$ and $\tau\omega \to \infty$, the second-order contribution $\Sigma_{ij}^{(2)}/\theta\partial_x u \approx \tau^2\theta/\delta^2 \to 0$, where δ is the width of the viscous layer.

By virtue of symmetry, the high powers of $\boldsymbol{S}$ disappear from the second-order relation (2.10). It is easy to see that this result is valid to all orders. Consider a general nth -order contribution to the rank-two stress tensor $\sigma_{x,y}$ of the kind

$$\xi_{x,y}^{(n)} = \frac{\partial u_{\alpha_1}}{\partial x_{\alpha_3}}\frac{\partial u_{\alpha_2}}{\partial x_y}\frac{\partial u_{\alpha_3}}{\partial x_{\alpha_{n-1}}}\cdots\frac{\partial u_x}{\partial x_{\alpha_n}}\cdots\frac{\partial u_{\alpha_{n-1}}}{\partial x_{\alpha_2}}\frac{\partial u_{\alpha_n}}{\partial x_{\alpha_1}} \tag{4.8}$$

where the summation is carried out over the randomly distributed Greek subscripts. Since $v = 0$ and $\partial_x u = 0$,

$$\frac{\partial u_x}{\partial x_{\alpha_n}}\frac{\partial u_{\alpha_n}}{\partial x_{\alpha_1}} = \frac{\partial u}{\partial y}\frac{\partial v}{\partial x_{\alpha_n}} = 0 \tag{4.9}$$

and we conclude that $\xi_{x,y}^{(n)} = 0$. This result, as a property of tensors of rank two formed from velocity derivatives in boundary layers where only $\partial_y u \neq 0$, is mentioned in Landau & Lifshitz (1981). Denoting $\sigma_{x,y} \equiv \sigma$, based on the above considerations, we obtain an equation valid in both low- and large-frequency limits:

$$\frac{\partial u}{\partial t} = -\frac{\partial \sigma}{\partial y}, \qquad \tau\frac{\partial \sigma}{\partial t} + \sigma = -\nu\frac{\partial u}{\partial y}. \tag{4.10a,b}$$

Comparing this result with (3.2), we conclude that constitutive equation (4.10) is a resummation of the Chapman–Enskog expansion used in the low-order derivation of (2.10). Indeed, the Fourier-transform of (4.10b) is equal to $(1 + \mathrm{i}\omega\tau)\sigma(y, \omega) = \nu\mathrm{d}u/\mathrm{d}y$ which in the limit $\omega\tau \to 0$, coinsides with (3.2). Equations (4.10) give

$$\tau\frac{\partial^2 u}{\partial t^2} + \frac{\partial u}{\partial t} = \nu\frac{\partial^2 u}{\partial y^2}. \tag{4.11}$$

Equation (4.11), derived here for the case of a rapidly oscillating plate, is the telegrapher's equation explored by Rosenau (1993).

https://doi.org/10.1017/S0022112007007148 Published online by Cambridge University Press

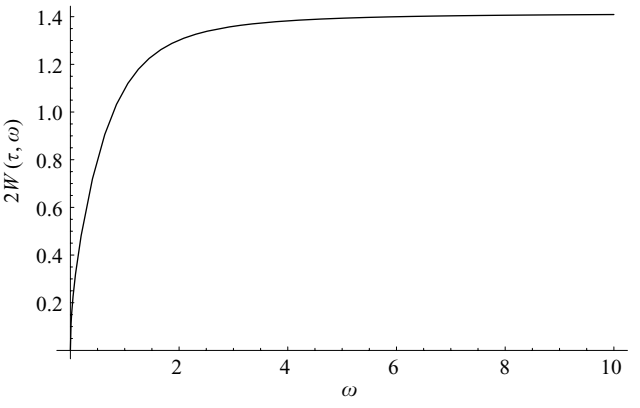


FIGURE 1. Dissipation rate $2W(\tau,\omega)$ as a function of ω (expression (4.16), arbitrary units).

Boundary conditions. Interested in the limit $\omega\tau > 1$, we have to be careful with the choice of boundary condition. The one used in this work is $u(0,t) = U(\omega\tau)\cos\omega t = \alpha(\omega\tau)U\cos\omega t$. The 'slip factor' has recently been investigated in detailed numerical simulations, where it was shown that for $\omega\tau \leqslant 1$, $\alpha(\omega\tau) \approx 1$ and it rapidly decreases to $\alpha(\omega\tau) \approx 0.3 - 0.2$ for $1 < \omega\tau \leqslant 100$ (Colosqui & Yakhot 2007; Alexander F. 2007, personal communication). Dealing with the linear equation, we can remove the slip factor from consideration by first introducing the normalized velocity field $u/U(\omega\tau)$, solve the equations and then recover $u(y,t)$.

Solution. The solution to equation (4.11) is found readily: $u = \mathrm{Re}[\mathrm{e}^{-\mathrm{i}\omega t}\mathrm{e}^{-y/\delta}]$ with $1/\delta = -(1-\mathrm{i})\sqrt{\omega/2\nu}\sqrt{1-\mathrm{i}\omega\tau}$ and

$$u = U\mathrm{e}^{-y/\delta_-}\cos(\omega t - y/\delta_+) \tag{4.12}$$

where

$$1/\delta_\pm = (1+\omega^2\tau^2)^{1/4}\sqrt{\omega/2\nu}\left[\cos\left(\tfrac{1}{2}\tan^{-1}(\omega\tau)\right) \pm \sin\left(\tfrac{1}{2}\tan^{-1}(\omega\tau)\right)\right]. \tag{4.13}$$

In the limit $\omega\tau \to 0$, this solution tends to (3.13) derived above. As we see, the non-Newtonian second Stokes problem can be characterized by two different length: scales: the penetration length δ_- and the wavelength δ_+. In the limit $\omega\tau \to \infty$, the penetration length tends to infinity and the dominating dissipation mechanism is wave generation. (This limits the velocity gradients in this problem.) To calculate the force acting on unit area of the plate, we notice that in accord with the differential equations (4.10):

$$\sigma(0,t) = \rho\nu\exp\left(-\frac{t}{\tau}\right)\int_{-\infty}^{t}\frac{\partial u(0,\lambda)}{\partial y}\exp\left(\frac{\lambda}{\tau}\right)\mathrm{d}\frac{\lambda}{\tau} \tag{4.14}$$

where $\nu\partial u(0)/\partial y = U(-(\cos\omega t)/\delta_- + (\sin\omega t)/\delta_+)$ and

$$\sigma(0,t) = \rho\nu\frac{U}{1+\omega^2\tau^2}\left[-\frac{1}{\delta_-}(\cos\omega t + \omega\tau\sin\omega t) + \frac{1}{\delta_+}(-\omega\tau\cos\omega t + \sin\omega t)\right] \tag{4.15}$$

where ρ is the density of a fluid. To obtain the dissipation rate per unit time per unit area of the plate, we calculate $W = -\overline{u(0,t)\sigma(0,t)}$ averaged over a single cycle:

$$W(\tau,\omega) = \frac{1}{2}\frac{\mu U^2}{1+\omega^2\tau^2}\left(\frac{1}{\delta_-} + \frac{\omega\tau}{\delta_+}\right). \tag{4.16}$$

A plot of the normalized dissipation rate as a function of $\omega\tau$ is shown on figure 1.

https://doi.org/10.1017/S0022112007007148 Published online by Cambridge University Press

As $\omega\tau \to 0$, we recover the previous result $W/\sqrt{\omega} \propto (1 + \frac{1}{2}\omega\tau)$. In the opposite limit $\omega\tau \to \infty$, saturation of the curve $W(\omega\tau)$ is predicted. In this range, the kinetic energy of the plate oscillations is mainly dissipated into wave radiation.

Described by (4.10), which in rheology is called the Maxwell model, viscoelastic phenomena are a well-known feature of flows of high-molecular-weight polymer solutions (for excellent reviews see Bird, Stewart & Lightfoot 2002; Brodkey 1967). Treating polymers as elastic springs, this model is usually phenomenologically introduced by the addition of elastic (Hookean) contributions, dominating the high-frequency properties of the stress tensor. This approach led to many important results, including (4.12), (4.13) (Bird *et al.* 2002). The viscoelasticity of polymer solutions can be attributed to their very large polymer-dominated relaxation times resulting in $Wi = \tau\omega > 1$ even in the moderately high-frequency flows which, according to the theory, are governed by (4.10). *It follows from our formulation that this feature is a general property of high-frequency fluid dynamics and one can safely conclude that all high-frequency low-Reynolds-number (Re* $\to 0$*) flows, where the inertial contributions are negligibly small, are rheological.* Except for the relaxation time approximation, no phenomenology and no ad hoc assumptions were involved in our derivation.

5. 'Plane oscillator'; nanoresonators

Consider a massless spring of stiffness k with two infinite plates of height h attached to it. The losses in the spring are neglected and the friction force, acting on the plates, is the only source of energy dissipation. The equation of motion of this 'plane oscillator" driven by a force $R(t)$ is

$$x_{tt} + \gamma x_t + kx = R(t) \tag{5.1}$$

where $\gamma x_t = \gamma u(0,t) = 2\rho\sigma(0,t)/m_s$ is the friction force acting on a unit mass ($m_s = \rho_p h$) of a plate surface and the factor 2 accounts for the force acting on both (top and bottom) surfaces of the plate. If the resonance $I(\omega_0)$ is sharp enough, so that $\delta\omega/\omega_0 \ll 1$, then we can calculate the damping (friction) force acting on the oscillator using the theory developed above. In the Newtonian limit (hereafter, we omit the subscript 0) $\omega\tau \to 0$, (4.15) gives $\gamma = \sqrt{\mu\rho\omega/(2m_s^2)} \propto \sqrt{\omega}$ and the quality factor (defined below) $Q \approx \omega/\gamma \propto \sqrt{\omega}$. In the opposite (kinetic) limit $\omega \to \infty$ and $\tau = \text{const}$: $\gamma \to \mu\omega\tau\sqrt{\omega/\nu}/(m_s(1+\omega^2\tau^2)^{3/4}) \propto \omega^0 = \text{const} = O(\rho c/m_s)$. Thus, in this limit the inverse quality factor $1/Q = \gamma/\sqrt{\omega^2 - \gamma^2} \approx \gamma/\omega \propto 1/\omega$. For a gas of a given temperature, $\rho \propto p$ and $c \propto \sqrt{\theta/m_{mol}} = \text{const}$, we have $1/Q \propto p/\omega$.

The relation, following from (4.15), valid in the entire range of frequency variation is:

$$\gamma = g\frac{\rho\sqrt{\omega_p\nu}}{\rho_p h(1+\omega^2\tau_p^2)^{3/4}}\left[(1+\omega\tau_p)\cos\left(\tfrac{1}{2}\tan^{-1}\omega\tau_p\right) - (1-\omega\tau_p)\sin\left(\tfrac{1}{2}\tan^{-1}\omega\tau_p\right)\right] \tag{5.2}$$

where the factor g, accounting for geometrical details of the device, will be discussed below. Our goal now is to find the relaxation time τ_p responsible for relaxation to equilibrium in the immediate vicinity of the rapidly oscillating solid plate. In a standard equilibrium situation, when λ and $\tau \approx \lambda/c \ll 1/\omega$ are the smallest length and time scales in the system, the relaxation times in the bulk and in the immediate vicinity of the surface are more or less equal. In a rapidly oscillating flow, such as we are interested in, this is not so. Indeed, even in air at normal conditions, the bulk $\tau \approx \lambda/c \approx 10^{-9}$ s and in modern microresonators, where $\omega \approx 10^9\,\text{s}^{-1}$, the inequality $\omega\tau \ll 1$ is hardly satisfied. Moreover, in the low-pressure devices where

https://doi.org/10.1017/S0022112007007148 Published online by Cambridge University Press

$\omega_0/2\pi$ (MHz)	Q_{Th} 800	Q_{Ex} 800	Q_{Th} 500	Q_{Ex} 500	Q_{Th} 300	Q_{Ex} 300	Q_{Th} 100	Q_{Ex} 100	Q_{Th} 50	Q_{Ex} 50
1.97	944	758	1185	962	1510	1299	2480	329	445	439
24.2	145	139	180	175	239	231	569	474	1102	787
102.5	338	292	500	443	803	641	2361	1493	4712	2703

TABLE 1. Comparison between experimental data and theoretical predictions of Q for pressures in the range 800 to 50 Toor.

$10^{-3} \leqslant p \leqslant 10^3$ Torr, the bulk relaxation time is huge, so that τ_p must be calculated from a theory taking into account strongly non-equilibrium effects. In the absence of such a theory, we use the results of experimental data on a driven microbeam obtained by Karabacak, Yakhot & Ekinci (2007) who covered an extremely wide range of parameter variation: $10^0 \leqslant p \leqslant 10^3$ Torr, $10^6 \leqslant \omega \leqslant 0.6 \times 10^9\ \mathrm{s}^{-1}$, $h = 2 \times 10^{-5}$ cm. Under the normal conditions for $\omega = 0.6 \times 10^9\ \mathrm{s}^{-1}$, the observed damping parameter was $\gamma \approx 1.5 \times 10^6\ \mathrm{s}^{-1}$. (This relation is the result of the measured $1/Q = \gamma/\omega \approx 3 \times 10^{-3}$ and $\omega_0 = 0.6 \times 10^9\ \mathrm{s}^{-1}$.)

Now we show that our theory, developed for the simplest possible flow geometry, is in a close agreement with experimental data on various nanoresonators. In nanotechnological applications, the $O(10^{-6}\,\mathrm{cm})$ amplitude of displacement is much smaller than the smallest linear dimension of a real beam or cantilever, widely used in applications. Therefore, the relations derived in this work may be not very geometry-sensitive. For example, the solution to the problem of an infinite cylinder oscillating along its axis can be expressed in terms of Bessel functions, leading to $O(1)$ variations of the coefficient g in front of (5.2). Here, to qualitatively illustrate the origins of the geometric factor g, we use very simple considerations. As stated above, the mass per unit area of a plate of height h and length l is $m_s = \rho_p l^2 h/l^2 = \rho_p h$. A simple calculation of m_s for a circular cylinder gives $m_s = \rho a/2$, where a is the radius. In this case, $g_{cyl} \approx 4 d_{plate}$. For a beam of height h and width w, we have $m_s = \rho_p wh/(2(w+h))$. Thus, the dissipation per unit area may be a relatively universal property (Karabacak *et al.* 2007). Choosing $g \approx 3$ and using the experimental data for normal pressure $p = 800$ Torr as a calibration point, we obtain $\tau_p(800\,\mathrm{Torr}) \approx 2.2$ ns (Karabacak *et al.* 2007). Then, based on kinetic theory, we substitute $\tau_p = 1850/p$ ns into (5.2) and obtain γ and quality factor $Q(\omega, p)$ in good agreement with the results data of Karabacak *et al.* (2007) in a wide range of both frequency and pressure variation ($10^6 \leqslant \omega \leqslant 0.6 \times 10^9$ Hz; $100 \leqslant p \leqslant 1000$ Torr.) It is interesting that all experimental data of Karabacak *et al.* (2007) on beams and cantilevers were successfully fitted by (5.2) with the geometric factor 2.8.

Comparisons between theoretical predictions based on (5.2) and experimental data are presented in figure 2 and table 1. The damping factor γ (Ekinci & Karabacak, 2007, personal communication), obtained from experiments on a cantilever operating at a relatively low frequency $\omega = 2\pi \times 309$ kHz, is compared with theoretical predictions in figure 2(b) for a wide range of pressure variation. The theoretically predicted transition, indicated on figure 2(b) by an arrow, from $Q \propto \omega$ in the low-pressure region, to $Q \propto \sqrt{\omega}$, is clearly seen. The transition point at $p \approx 3-4$ Torr (see figure 2b) corresponding to $\tau\omega \approx 1850\omega/p \approx 1$, is well correlated with the theoretical curve (solid line). The data on high-frequency double-clamped beams, covering a wide range of pressure variation ($50 \leqslant p \leqslant 800$ Torr), are shown in table 1.

https://doi.org/10.1017/S0022112007007148 Published online by Cambridge University Press

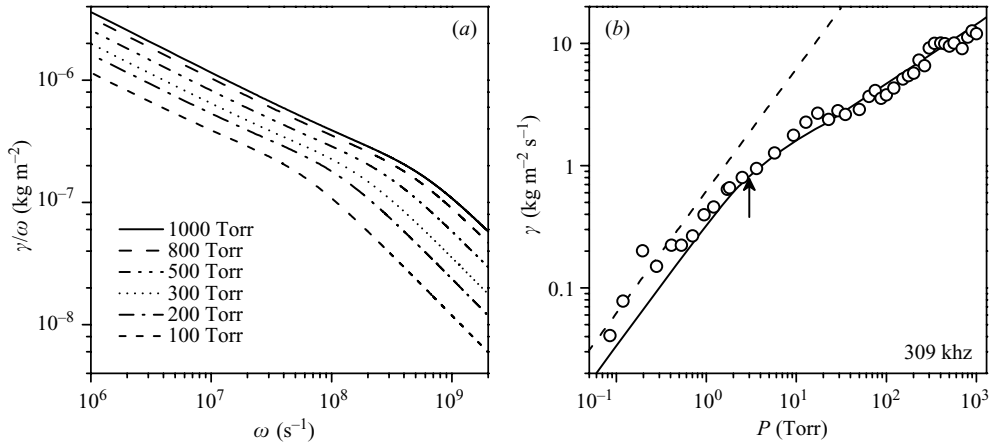


FIGURE 2. (*a*) Theoretical inverse quality factor $1/Q_{th} \approx \gamma/\omega$ vs ω (formula (5.2)) in the pressure interval $100 < p < 1000$ Torr. Relaxation time $\tau_p(800\,\text{Torr}) = 2.2$ ns. For remaining parameters, see text. (*b*). Comparison of theoretical and experimental Q_{th} and Q_e quality factors for a cantilever at $\omega = 2\pi \times 309$ kHz and $0.1 \leqslant p \leqslant 800$ Torr. (Ekinci & Karabacak, 2007, personal communication). Solid curve, theory; circles, experimental data. Broken line shows non-Newtonian asymptotics $Q \propto \omega$.

In the limit $p \to 0$, the only relevant dissipation is due to the inelastic solid-state effects within the resonator. Thus, to assess the fluidic dissipation, dominating the high-pressure regime, this residual damping must be subtracted from the total dissipation rate. This procedure, introducing some inaccuracy in the low-pressure range, has been applied by Karabacak *et al.* (2007). Variation of the operating frequency has been achieved by manufacturing devices of widely varying linear dimensions. This complex fabrication process, limiting the number of available samples used in the averaging procedure, leads to an additional statistical scattering of the data. Still, neglecting a very few data points, corresponding to the anomalously large deviations, the deviation of theoretical predictions from experimental data was within $10\,\% - 20\,\%$. A more extensive comparison of the theory with experiments, covering different devices, can be found in Karabacak *et al.* (2007).

In a dense liquid where $\omega\tau \ll 1$, relation (5.2) gives $\gamma = g\rho\sqrt{\omega\nu}/\rho_p h$ and in water ($\nu \approx 0.01\,\text{cm}^2\,\text{s}^{-1}$, $\rho_p/\rho \approx 2$, $\omega \approx 0.6 \times 10^9\,\text{s}^{-1}$; $h = 2 \times 10^{-5}$ cm and $w = 7 \times 10^{-5}$ cm, $g \approx 2 - 3$), corresponding to the experimental set up of Verbridge *et al.* (2006), we predict $\gamma \approx 1.2 - 1.8 \times 10^8\,\text{s}^{-1}$ and $Q \approx \sqrt{\omega^2 - \gamma^2}/\gamma \approx 3.5 - 5$, in a good agreement with $Q \approx 4 - 5$, experimentally observed by Verbridge *et al.* (2006).

6. Summary and conclusions

A solution to the Boltzmann–BGK equation, for the problem of a flow generated by an oscillating plate, valid in a wide range of dimensionless frequency variation $0 \leqslant \omega\tau \leqslant \infty$, is presented. This solution describes the experimentally observed transition between viscoelastic ($\tau\omega \ll 1$) and purely elastic ($\tau\omega \gg 1$) regimes. The results obtained for a simple 'plane oscillator', first introduced in this paper, are in close agreement with experiments on nanoresonators operating in an extremely wide range of pressure and frequency variation in both gases (Ekinci & Karabacak 2007, personal communication; Karabacak *et al.* 2007) and in water (Verbridge *et al.* 2006).

https://doi.org/10.1017/S0022112007007148 Published online by Cambridge University Press

The relative insensitivity of the results to geometrical details of nanoresonators may prove important for future numerical simulations of these important devices.

We would like to thank K. Ekinci and D. Karabacak for sharing with us their yet unpublished data on microresonators. We benefited from the most interesting and stimulating discussions with them and R. Benzi, H. Chen, R. Zhang, X. Shan, F. Alexander, S. Succi, I. Karlin, V. Steinberg and H. Stone.

REFERENCES

Benzi, R., Succi, S. & Vergassola, M. 1992 The lattice Boltzmann equation: theory and applications. *Phys. Rep.* **222**, 145.

Bhatnagar, P. L., Gross, E. & Krook, M. 1954 A model for collisions in gases I. Small amplitude processes in charged and neutral one-component systems. *Phys. Rev.* **94**, 511–525.

Binning, C., Quate, C. F. & Gerber, C. 1986 Atomic force microscope. *Phys. Rev. Lett.* **56**, 930–933.

Bird, R. B., Stewart, W. E. & Lightfoot, E. R. E. 2002 *Transport Phenomena*, 2nd Edn. Wiley and Sons.

Brodkey, R. S. 1967 *The Phenomena of Fluid Motions.* Dover.

Chen, H., Kandasamy, S., Orszag, S. A., Shock, R., Succi S. & Yakhot, V. 2003 Extended Boltzmann kinetic equation for turbulent flows. *Science* **301**, 633–636.

Chen, H., Orszag, S. A., Staroselsky, I. & Succi, S. 2004 Expanded analogy between Boltzmann kinetic theory of fluids and turbulence. *J. Fluid Mech.* **519**, 301–313.

Chen, S. Y. & Doolen, G. 1998 Lattice Boltzmann method for fluid flows. *Annu. Rev. Fluid Mech.* **30**, 329–xxx.

Cleland, A. N. & Roukes, M. L. 1998 A nanometer-scale mechanical electrometer. *Nature* **392**, 160–162.

Colosqui, C. & Yakhot, V. 2007 Lattice Boltzmann simulations of second Stokes flow problem. *J. Mod. Phys.* (in press).

Ekinci, K. L., Huang, X. M. & Roukes, M. L. 2004 Ultrasensitive mass detection. *Appl. Phys. Lett.* **84**, 4469.

Karabacak, D. M., Yakhot, V. & Ekinci, K. L. 2007 High frequency nanofluidics: experimental study with nano-mechanical resonators. *Phys. Rev. Lett.* (in press) (ArXiv, cond-mat/0703230).

Landau, L. D. & Lifshitz, E. M. 1959 *Fluid Mechanics.* Pergamon.

Landau, L. D. & Lifshitz, E. M. 1981 *Physical Kinetics.* Butterworth-Heinemann.

Rosenau, P. 1993 Random walker and the telegrapher's equation: A paradigm of generalized hydrodynamics. *Phys. Rev.* E **48**, R655-657.

Service, R. B. 2006 Tipping scales - just barely. *Science* **312**, 683.

Stokes, G. G. 1851 On the effect of the internal friction in fluids on the motion of pendulums. *Camb. Phil. Trans.* **IX**, 8.

Verbridge, S. S., Bellan, L. M., Parpia, J. M. & Craighead, H. G. 2006 Optically driven resonance of nanoscale flexural oscillators in fluids. *Nano Lett.* **6**, 2109–2114.

https://doi.org/10.1017/S0022112007007148 Published online by Cambridge University Press